Integrated Sensing and Actuation Capabilities of Flexible Surface Acoustic Wave Devices with Metallic and Polymer Layers

Shahrzad Zahertar[1], Ran Tao[1,2], Hamdi Torun[1], Pep Canyelles-Pericas[1,3], Yong-Qing Fu[1]

[1]Department of Mathematics, Physics, and Electrical Engineering, Northumbria University, Newcastle upon Tyne, UK
[2]Shenzhen Key Laboratory of Advanced Thin Films and Applications, College of Physics and Optoelectronic Engineering, Shenzhen University, China
[3]Department of Integrated Devices and Systems, University of Twente, Enschede, Netherlands
s.zahertar@northumbria.ac.uk

***Abstract*— Flexible and bendable devices have become the key elements in the development of next-generation point-of-care systems and wearable technologies. In this paper, we report flexible surface acoustic wave (SAW) devices that are composed of a multilayer substrate; SAW devices are basically made of interdigital transducers (IDTs) that are patterned on a piezoelectric layer. In our fabricated devices, thin film of zinc oxide (ZnO), as the piezoelectric layer, is deposited on substrates made of trilayer of thin metal films (Nickel/Copper/Nickel) on top of a polyethylene terephthalate (PET) layer. We have characterized the devices in radio frequencies, and we have measured the response of the device to the temperature and the Ultraviolet (UV) light. Also, we have tested the actuation capability of our fabricated devices. We have successfully demonstrated that our fabricated devices can be employed as an integrated platform for sensing and actuation purposes using a single structure.**

Keywords—Surface Acoustic Waves; Microfluidic Actuation;

I. INTRODUCTION

The main objective in development of Lab-on-chip (LOC) devices is to bring the whole laboratory process onto a small chip. These devices are capable of performing multiple functions including sample preparation, actuation, and sensing. Therefore, achieving a successful LOC device is challenging and usually requires integration of various platforms [1], [2].

Surface acoustic wave (SAW) sensors and actuators are capable of generating and detecting acoustic waves confined in the substrate using interdigital transducers (IDTs) that are patterned on a piezoelectric layer [3], [4]. SAW devices have been extensively studied for their capabilities in sensing and as well as in microfluid manipulation such as streaming, pumping, jetting and nebulization [5]–[8]. Therefore, having both functionalities of sensing and actuation, these devices are attractive to be integrated into lab-on-chip platforms.

II. FABRICATION AND METHODOLOGY

A. Fabrication

The IDTs made of Cr/Au layers with thicknesses of 20/100 nm and various wavelengths, λ, of 64, 100, and 160 µm were patterned on a multi-layered substrate through standard photolithography and lift-off processes. The substrate of the fabricated devices is made of ZnO/Ni/Cu/Ni/PET with the thicknesses of 5, 1, 23, 1, 125 µm for each layer respectively. Ni/Cu/Ni film is commercially available and is obtained from Shenzen Vanlead Technology Co. LTD., China. ZnO was deposited on the substrates using a direct current (DC) magnetron sputter. Thickness of ZnO film was controlled to be ~5 µm and uniformity was achieved by rotating the sample holders during the deposition process. The substrate was bonded to the PET layer by roll-to-roll process.

B. Experimental method

The IDT electrode pads were connected to one port of vector network analyzer (Keysight N9913A) for device characterization and reflection spectra of the fabricated devices were obtained. During temperature sensing experiments, the samples were placed in an oven and temperature of the oven was varied from room temperature up to 100 °C. The temperature was also carefully monitored with a temperature sensor that was attached on top of the acoustic wave devices. To evaluate the effect of the wavelength of the IDTs on the response of the fabricated devices to the UV light, the devices were connected to the vector network analyzer and placed under a UV gun (CS2010; Thorlabs Inc.,Newton, NJ). UV intensity of 151.2 mW/cm^2 for the duration of 22 seconds was applied to perform the experiments. The wavelength of the UV light is 365 nm. A LabVIEW (National Instruments Inc.) based program was developed to implement real-time measurements of frequency changes of the flexible SAW UV sensors. Fig. 1 represents a schematic of a fabricated device and the layers in the substrate.

For performing microfluidic actuation experiments, the surface of the device was hydrophobically treated with 1% CYTOP solution (L809-A). A signal generator (Marconi Instruments 2024) was utilized to calibrate the frequency and its output was fed to an amplifier (Amplifier Research, 75A250). The output of the amplifier was then connected to the electrode pads of the SAW device. A droplet of 1 µL of deionised water (DI) was placed in front of the IDTs, and the droplet movement was captured using a conventional CMOS camera.

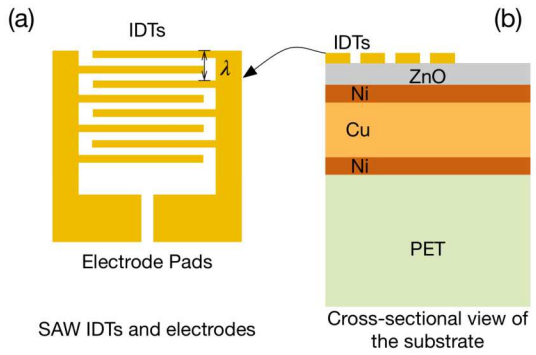

Fig 1. Schematic of the (a) structure of the surface acoustic wave device and (b) cross-sectional view of the fabricated devices

III. Device Characterization

Fundamental SAW frequency of the devices depends on the wavelength of the IDTs and the phase velocity of acoustic waves in the substrate ($f=v/\lambda$, f as the fundamental resonance, v as the phase velocity of acoustic waves in the substrate, and λ is the wavelength of IDTs). The resonances of a SAW device can be identified by connecting the electrode pads of the structure to one port of a vector network analyzer and by monitoring the reflection coefficient (S_{11}). Fig. 2 represents the S_{11} spectra of the fabricated devices with IDTs of various wavelengths of 64, 100, 160 µm. As can be seen from Fig. 2, by increasing the wavelength, the resonant frequencies shift towards lower values. Lamb waves are usually generated in thin structures, where the thickness of the substrate is smaller than the designed wavelength. There are two types of lamb waves that can be present in thin film membrane, (a) anti-symmetric (A-mode) or (b) symmetric (S-mode) [9]–[11]. These modes are labelled in Fig. 2. The first resonant frequency is asymmetric lamb wave (A_0), the second resonant frequency is symmetric lamb wave (S_0) mode, and the subsequent frequencies (if any) are higher order asymmetric and symmetric resonant modes of lamb waves.

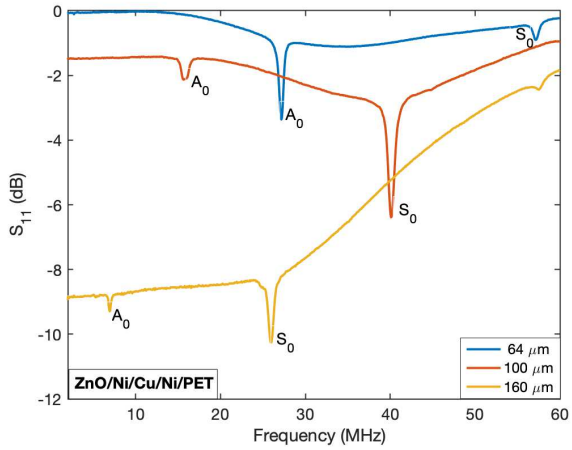

Fig. 2. Reflection coefficient of fabricated devices with various wavelengths (64, 100, and 160 µm) of IDTs

IV. Sensing Capability

SAW devices can easily be integrated into various platforms for sensing applications. The resonant frequency of a SAW device depends on the phase velocity of acoustic waves in the substrate and there are multiple factors that can influence and alter the phase velocity including temperature, mass loading, pressure, conductivity etc., resulting in a change in the resonant frequency ($\Delta f/f = \Delta v/v$) [5]. Monitoring the shift in the resonant frequency caused by these factors can be utilized as a sensing mechanism.

A. Responsiveness to temperature change

Temperature can have a significant effect on SAW devices composing of a polymer substrate, e.g. PET, and this phenomenon can have applications where maintaining a constant temperature is very critical for device performance in integrated platforms. That is because by employing polymer substrates, the change in temperature can easily be identified. Temperature coefficient of frequency or TCF (TCF = $(\Delta f/(f\Delta T)$, where Δf is the change in frequency, ΔT is the change in temperature respectively), which is a measure of change in frequency relative to a reference frequency with varying temperature, is an aspect of monitoring the response of the device to the temperature change. To obtain the TCF values, samples were placed in an oven and resonant frequencies of the devices were monitored while temperature was increased.

Fig. 3 shows the values of TCF for our fabricated devices with different wavelengths of IDTs.

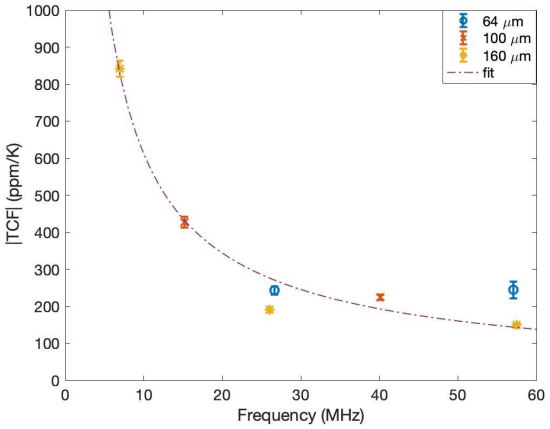

Figure 3. Temperature coefficient of frequency of the fabricated devices with various wavelengths of IDTs

As illustrated in Fig. 3, it is possible to achieve very high values of TCF with the fabricated devices. The highest value achieved was for the device with IDT wavelength of 160 µm and when it was calibrated at its lowest resonant frequency mode. The obtained TCF value in this case was 822 ppm/K. For lower wavelengths of IDTs, the achieved TCF value was also lower.

B. *Responsiveness to UV exposure*

Previously, we showed how changing the intensity of UV light can increase the conductance in ZnO layer, and therefore, lead to a change in the resonant frequency of the SAW device [12]. In this paper, for our next set of experiments, we investigated the effect of wavelengths of IDTs on the response of the device to the UV light. We exposed the fabricated devices to the UV intensity of 151.2 mW/cm^2 (maximum intensity of the UV gun) for the duration of 22 seconds and monitored the change in value of resonant frequencies for each wavelength. The results are show in Fig. 4.

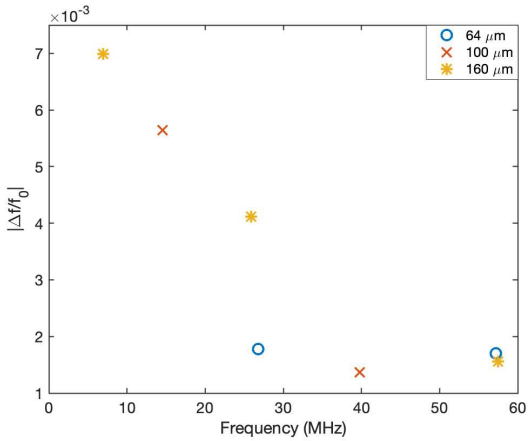

Fig. 4. Comparison of UV-responsiveness of fabricated devices with various wavelengths of IDTs

The devices with higher wavelengths of IDTs calibrated at their lowest resonance showed a more significant response to the UV exposure, while all the devices showed weaker response to UV-exposure when calibrated at their higher resonances.

V. Actuation Capability

Next, we investigated the possibility of pumping sessile droplets in micro-volumes using our fabricated device. Device with wavelength of 160 µm was selected for performing the experiments. Fig. 5 shows the pumping velocities of a 1 µL droplet when signal generator was calibrated at 8.2 MHz and power was applied to electrode pads of the SAW device. Pumping of the droplet could be achieved for the powers of 1.8 W up to 4.6 W as shown in Fig. 5. The pumping speed was initially 0.008 mm/s for the power of 1.8 W, and it reached its maximum of 0.52 mm/s at the applied power of 3.6 W. After this point, further increasing the RF power led to lower speed for pumping, which could be a result of energy that is converted to heat and is lost in the substrate at such higher powers.

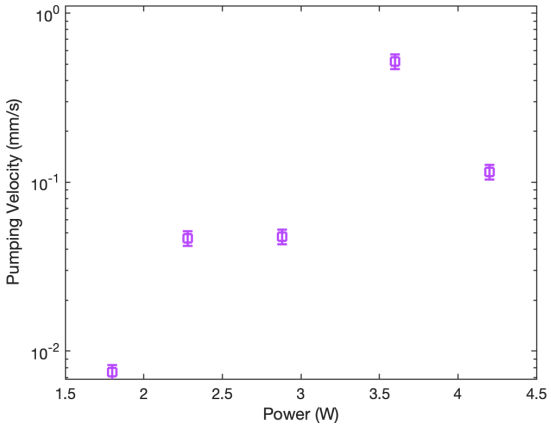

Fig. 5. Pumping velocity versus different applied powers of a 1 µL droplet, which was placed in front of the fabricated device with IDT wavelength of 160 µm.

Therefore, the nonlinearity observed in Fig. 5 can be attributed to the heating effect caused by substantial increase of the power and its dissipation into the polymer substrate.

VI. Conclusions

In this paper, we have reported a flexible surface acoustic wave device which can be used as an integrated platform for sensing and actuation purposes. We have tested the response of the fabricated devices to the temperature variance, and we have investigated the effect of wavelength of IDTs on device's responsiveness to the UV exposure. Finally, we have investigated the actuation capability of our proposed device on pumping a sessile droplet. Our results indicate that these structures have the potential to be effectively integrated in the next-generation of point-of-care devices.

Acknowledgment

The This work was supported by the Engineering Physics and Science Research Council of UK (EPSRC EP/P018998/1) and UK Fluidic Network (EP/N032861/1) - Special Interest Group of Acoustofluidics.

REFERENCES

[1] L. R. Volpatti and A. K. Yetisen, 'Commercialization of microfluidic devices', *Trends in Biotechnology*, vol. 32, no. 7, pp. 347–350, Jul. 2014, doi: https://doi.org/10.1016/j.tibtech.2014.04.010.

[2] S. K. Vashist, P. B. Luppa, L. Y. Yeo, A. Ozcan, and J. H. T. Luong, 'Emerging Technologies for Next-Generation Point-of-Care Testing', *Trends Biotechnol*, vol. 33, no. 11, Art. no. 11, Nov. 2015, doi: 10.1016/j.tibtech.2015.09.001.

[3] J. F. Tressler, S. Alkoy, and R. E. Newnham, 'Piezoelectric sensors and sensor materials', *Journal of electroceramics*, vol. 2, no. 4, pp. 257–272, 1998.

[4] J. W. Grate, S. J. Martin, and R. M. White, 'Acoustic wave microsensors', *analytical Chemistry*, vol. 65, no. 21, pp. 940A-948A, 1993.

[5] Y. Q. Fu *et al.*, 'Advances in piezoelectric thin films for acoustic biosensors, acoustofluidics and lab-on-chip applications', *Progress in Materials Science*, vol. 89, pp. 31–91, Aug. 2017, doi: 10.1016/j.pmatsci.2017.04.006.

[6] S. Zahertar, Y. Wang, R. Tao, J. Xie, Y. Q. Fu, and H. Torun, 'A fully integrated biosensing platform combining acoustofluidics and electromagnetic metamaterials', *J. Phys. D: Appl. Phys.*, vol. 52, no. 48, p. 485004, Nov. 2019, doi: 10.1088/1361-6463/ab3f7d.

[7] A. Wixforth, 'Acoustically driven programmable microfluidics for biological and chemical applications', *JALA: Journal of the Association for Laboratory Automation*, vol. 11, no. 6, pp. 399–405, 2006.

[8] R. Tao *et al.*, 'Integrating microfluidics and biosensing on a single flexible acoustic device using hybrid modes', *Lab on a Chip*, vol. 20, no. 5, pp. 1002–1011, 2020.

[9] J. W. Grate, S. W. Wenzel, and R. M. White, 'Flexural plate wave devices for chemical analysis', *Analytical Chemistry*, vol. 63, no. 15, pp. 1552–1561, 1991.

[10] T. Laurent, F. O. Bastien, J.-C. Pommier, A. Cachard, D. Remiens, and E. Cattan, 'Lamb wave and plate mode in ZnO/silicon and AlN/silicon membrane: Application to sensors able to operate in contact with liquid', *Sensors and Actuators A: Physical*, vol. 87, no. 1–2, pp. 26–37, 2000.

[11] R. M. Moroney, R. M. White, and R. T. Howe, 'Microtransport induced by ultrasonic Lamb waves', *Applied physics letters*, vol. 59, no. 7, pp. 774–776, 1991.

[12] R. Tao *et al.*, 'Flexible and Integrated Sensing Platform of Acoustic Waves and Metamaterials based on Polyimide-Coated Woven Carbon Fibers', *ACS sensors*, vol. 5, no. 8, pp. 2563–2569, 2020.